THE 3-D TRUNCATION FILTERING METHODOLOGY DEFINED FOR PLANAR AND SPHERICAL MODELS: INTERPRETING GRAVITY DATA GENERATED BY POINT MASSES.

PETER VAJDA[1] AND PETR VANÍČEK[2]

ABSTRACT

This paper focuses on one particular way of linear filtering the gravity data to facilitate gravity inversion or interpretation. With the use of integral transforms the gravity anomalies are transformed into new quantities that allow an easier interpretation with the help of pattern recognition. As the integral transforms are in fact filters, and as the regions of integration are caps with a variable radius, which can be systematically changed as a free parameter, we refer to such methodology as the truncation filtering. Such filters may be understood as weighted spherical windows moving over the surface, on which the gravity anomaly is defined, the kernel of the transform being the weight function. The objective of this paper is to define and deploy the truncation filtering for a planar model, i.e. for a homogenous horizontally infinite layer with embedded anomalous masses, and for a spherical model, i.e., for a homogenous massive sphere with embedded anomalous masses. Instead of the original gravity anomaly, the quantities resulting from the truncation filtering are interpreted/inverted. As we shall see, this approach has certain benefits. The fundamental concept of the truncation filtering methodology is demonstrated here in terms of the model consisting of one point mass anomaly.

The relationship between the depth of the point mass and the instant of the onset of the dimple pattern observed in sequences produced by truncation filtering the synthetic gravity data generated by point masses is, for both the planar and spherical models, compiled by computer simulations, as well as derived analytically. It is shown, that the dimple pattern is a consequence of truncating the domain of the filter and is free of the choice of the kernel of the filter. It is shown, that in terms of the mean earth and depths of point masses no greater than some 100 km the spherical model may be replaced by a planar model from the perspective of the truncation filtering methodology. It is also shown, that from the viewpoint of the truncation filtering methodology the rigorous gravity anomaly may be approximated by the vertical component of the gravity disturbance. The relationship between the instant of the dimple onset and the depth of the point mass thus becomes linear and independent of the magnitude (mass) of the point mass.

Keywords: inverse problem, gravity inversion, gravity data interpreting, planar approximation, dimple onset, point mass

---

1 Geophysical Institute, Slovak Academy of Sciences, Dúbravská cesta 9, 842 28 Bratislava, Slovakia (geofvajd@nic.savba.sk)

2 Department of Geodesy and Geomatics Engineering, University of New Brunswick, Fredericton, N.B., Canada (vanicek@unb.ca)

1. TRUNCATION FILTER

By the *truncation filter* we understand any linear filter defined by a convolution of the gravity anomaly Δg (or eventually of the gravity disturbance), given on a reference surface (plane, sphere), with a weight function (kernel) w in a cap (a circle in the plane or a spherical cap on the sphere)

$$Z^{s_0}(P) = \iint_{C(s_0)} \Delta g(Q) w(P,Q) d\sigma_Q \ . \tag{1}$$

The radius s_0 of the cap C is a free parameter and is referred to as the *truncation parameter* (planar truncation parameter for the circle, radial truncation parameter for the spherical cap). The kernel is a function of the distance (planar distance or radial distance) between the computation point P (point of evaluation of the transformed quantity Z) and the variable integration point Q, at which Δg is given. The properties of Z and the shape of its surface depend on the type and definition of the gravity anomaly that is filtered, as well as on the chosen weight function. The shape of the surface of Z depends also on the value of the truncation parameter, that is why the superscript. The integration is carried out over surface elements $d\sigma_Q$.

2. TRUNCATION FILTERING METHODOLOGY

The truncation filter is used so, that the cap with a pre-selected size glides over the reference plane or sphere like a moving spherical window and transforms the gravity anomaly into quantity Z. Then the Z quantity is interpreted (inverted) instead of the original gravity anomaly. What is the benefit of interpreting/inverting the transformed quantity rather than the gravity anomaly itself? Note that the truncation filter has one free parameter, the truncation parameter, that enables computing a sequence (of surfaces or profiles) of Z with gradually changing (decreasing or increasing) the value of the truncation parameter. When animating such a sequence, using an analogy between the truncation parameter and time, dynamic patterns are observed in the sequence, that are signatures of the anomalous masses that generate the gravity anomaly, from which the Z sequence is computed. The sequences that are animated using computer visualization are for practical reasons presented as several subsequent "timeframes of the animation" in one plot, as it is not possible to present an animation in a paper.

It is even more transparent to study patterns in the sequence of (surfaces or profiles of) the first derivative of the Z quantity with respect to the truncation parameter

$$\frac{dZ^{s_0}}{ds_0} = \lim_{\Delta s_0 \to 0} \frac{Z^{s_0+\Delta s_0} - Z^{s_0}}{\Delta s_0} , \tag{2}$$

which is numerically computed by differencing the Z quantity at the consecutive values of the truncation parameter and dividing the difference by the step in the truncation parameter. The sequence of the first derivative of Z, which represents the change in the Z quantity with changing the truncation parameter, yields more pronounced patterns.

In general, each pattern depends on the mass anomaly generating it and on the type of the Z quantity - by the type we understand the choice of the weight function and the type of the gravity anomaly. Different Z quantities may be more or less suitable for identifying/interpreting different features of the anomalous mass distribution. From the instant - a particular value of the truncation parameter in the animation - of the onset of some patterns, depth determinations, or estimates thereof, may be obtained for certain mass anomalies. The link between the mass anomalies and the patterns can be established through computer simulations (modelling).

We demonstrate the methodology of interpreting/inverting the Z quantity, and particularly its change represented by dZ^{s_0}/ds_0, i.e. the methodology of interpreting gravity data by means of the truncation filtering - *the truncation filtering methodology*, on a point mass anomaly embedded at depth d in an infinite massive horizontal layer, and in a massive sphere.

3. THE 3-D TRUNCATION FILTERING FOR A PLANAR MODEL

In practical geophysical applications very often the gravity anomalies are referred to a planar model. For the planar model the truncation filter is defined as follows:

$$Z^{s_0}(x_P, y_P) = \int_0^{s_0} \int_0^{2\pi} \Delta g(x, y) w(s) s \, d\alpha \, ds \,, \tag{3}$$

where s is the planar distance between points P and Q,

$$s = \sqrt{(x - x_P)^2 + (y - y_P)^2} \,, \tag{4}$$

s_0 is the (planar) truncation parameter (radius of the integration circle), α is the angle between point Q and arbitrary reference point as viewed from point P, $d\sigma_Q = s \, ds \, d\alpha$ is the surface element, and the w kernel (the weight function) is chosen arbitrarily. It could be for instance

$$w(s) = k \,, \tag{5a}$$

where k is an arbitrary constant,

$$w(s) = e^{-s^2/a^2} \,, \tag{5b}$$

where a is arbitrary constant, or any other. Note that the choice of weight function specifies the filter properties of the truncation filter. It is a good idea to choose a kernel that is positive on the $\left\langle 0, s_0^{\max} \right\rangle$ interval, where $s_0^{\max}$ is the largest pre-selected value of the truncation parameter to be used in filtering the gravity anomaly, i.e., a kernel that does not have a node. The reason for choosing a kernel with no node will be justified later on. Anyhow, this is a recommendation only, not a requirement.

3.1. One point mass

Now let us select a simple model consisting of a point mass m placed at depth d below the surface of a horizontally infinite layer of volume density ρ_0 and thickness H greater than d (cf. Fig. 1).

Such a planar model of one point mass anomaly produces a gravity anomaly defined as the difference between the magnitude of the actual gravity attraction on the geoid and the magnitude of the normal attraction on the reference plane (the surface of the horizontal layer). The actual gravity attraction is the superposition of the attraction of the point mass and of the attraction of the infinite horizontal layer. The term "geoid" is artificial in the context of this model, still we will use it by analogy to the geoid used in geodesy. It shall be defined with help of the disturbing potential. Similarly, for this model, the reference plane shall become the equivalent to the reference ellipsoid used in geodesy. The disturbing potential T is the difference between the actual gravitational potential and the normal potential. The potential of the infinite layer is chosen for the normal potential. Although it is infinite, it will not prevent us from computing the disturbing potential. The actual gravitational potential is the sum of the potential of the point mass and the potential of the infinite layer. Consequently the disturbing potential is the Newtonian potential of the point mass. The geoid is defined by Bruns's formula (e.g. *Vaníček and Krakiwsky, 1986, page 493, eqn. (21.4)*), which is applicable to this model. Although the potential of the infinite layer is infinite, its first derivative with respect to the vertical to its surface, i.e. its attraction, is finite and constant on the surface and above (e.g. *Grant and West, 1965, page 239*, or *Kellogg, 1929*). Introducing a Cartesian coordinate system with the z-axis vertical to the surface of the infinite layer and oriented outward, with the origin straight above the point mass location, and furthermore using the distance r from the origin

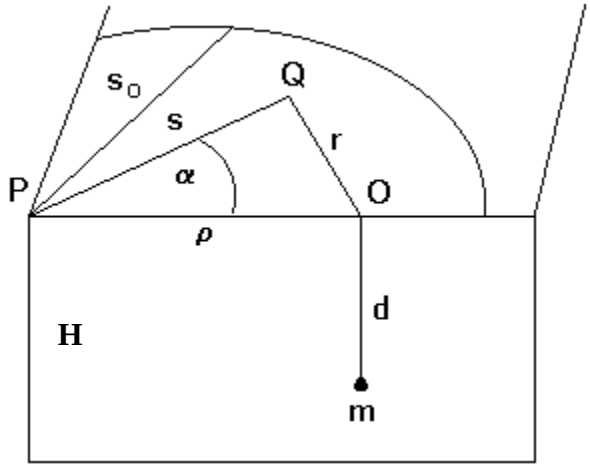

Fig. 1. The anomalous point mass m embedded at depth d in an infinite horizontal layer of thickness H.

instead of the x and y coordinates ($r^2 = x^2 + y^2$), we can write for the geoid, N being the geoidal height,

$$N(r) = \frac{T(r, z = N(r))}{\gamma} = \frac{m}{2\pi H \rho_0} \frac{1}{\sqrt{r^2 + (d + N(r))^2}}, \tag{6}$$

since the Bruns's formula requires that the disturbing potential is given on the geoid, where the disturbing potential is the Newtonian potential of the point mass

$$T(r, z) = \frac{\kappa m}{\sqrt{r^2 + (d + z)^2}}, \tag{7}$$

where κ is the gravitational constant, and the normal gravity ($\gamma = |\vec{\gamma}|$) reads

$$\gamma = 2\pi\kappa H \rho_0 . \tag{8}$$

The problem with the requirement on the disturbing potential to be given on the geoid which is sought can be dealt with by an iterative procedure by feeding the Bruns's formula with the disturbing potential given on the reference plane first ($N(r) = 0$) and then iterating it. This procedure converges very quickly. For our sake here the first iteration will be satisfactory.

Once the geoid is known, the gravity anomaly can be evaluated as

$$\Delta g(r) = |\vec{g}(r, z = N(r)) + \vec{\gamma}(r, z = N(r))| - \gamma . \tag{9}$$

Note that $\vec{\gamma}$ is constant and perpendicular to the reference surface (oriented downward) everywhere on and above the surface.

Now we adopt the first approximation to be used in this paper, namely we replace the actual gravitational attraction on the geoid by the actual gravitational attraction on the reference surface

$$\Delta g(r) \doteq |\vec{g}(r, z = 0) + \vec{\gamma}(r, z = 0)| - \gamma , \tag{10}$$

which rewritten in components reads

$$\Delta g(r) \doteq \sqrt{g_r^2(r, z = 0) + (g_z(r, z = 0) + \gamma)^2} - \gamma . \tag{11}$$

Next we adopt the second approximation to be used in this paper, that is we neglect the g_r^2 term, as

$$g_r^2 << (g_z + \gamma)^2 ,$$

which is justifiable in all cases when the attraction of the point mass is perturbing rather than comparable with respect to the attraction of the infinite horizontal layer. The second approximation results in

$$\Delta g(r) \doteq g_z(r, z=0) = \frac{\kappa m d}{\left(r^2 + d^2\right)^{3/2}} . \tag{12}$$

Rigorously these two approximations mean, that the gravity anomaly is approximated by the vertical (z) component of the gravity disturbance. Below we shall assess such an approximation by numerical experiments. There is another way of defining the gravity anomaly, namely from the fundamental gravimetric equation (e.g., *Vaníček and Krakiwsky, 1986, page 495, eqn. (21.14)*). This is neither needed nor adopted in the context of this paper. The interested reader is referred to e.g. *Vaníček et al. (1999)*.

3.1.1. Dimple onset - computer simulation

We may now compute the surface of the gravity anomaly, approximated by the vertical component of the gravity disturbance (eqn. (12)), generated by a point mass and truncation filter this gravity anomaly, while choosing the kernel of eqn.(5b). To truncation filter a gravity anomaly means to transform the surface of the gravity anomaly into the sequence of surfaces of Z^{s_0} and dZ^{s_0}/ds_0 for a pre-selected sequence of values of the truncation parameter $s_0^{(1)}$ to $s_0^{(n)}$ with a step of Δs_0. The two sequences are referred to as the Z sequence, and the dZ/ds_0 sequence, respectively. We do not present the Z sequence generated by our point mass in a graphical plot here, as it does not show much interesting behavior. Let us take a look at the dZ/ds_0 sequence, produced by our point mass, instead, see Fig. 2.

The dZ/ds_0 sequence displays a pattern of a dimple, i.e. the convex profile while collapsing develops a dimple (a pit) at a certain instant (a particular value of the truncation parameter) that continues to spread during the collapse of the profile (compare also to *Vajda and Vaníček, 1997;1999*). The dimple sets on in the sequence at a particular value of the truncation parameter, referred to as the *instant of the dimple onset*, denoted as s_0^*. Computer simulations for several different depths and masses (such that the amplitude of the geoidal height would not exceed 100 meters) of the point mass and for several different choices of the kernel of the truncation filter have revealed, that, although the shape of the Z quantity and of its first derivative, and hence the shape of the dimple pattern, depend on the choice of the kernel and on the depth of the point mass, the instant of the dimple onset is independent of the choice of the kernel. This fact will be justified below analytically. Moreover, computer simulations have revealed, that s_0^* is independent of the magnitude m of the point mass anomaly and depends linearly on its depth as $s_0^* \doteq 0.82\, d$. This is an interesting observation that has direct application in terms of gravity interpreting/inversion – when the gravity anomaly generated by one point mass is filtered by the truncation filter, the depth of the point mass is directly determined from the instant of the dimple onset in the sequence of the first derivative of Z as $d \doteq 1.22\, s_0^*$. Below we justify this statement analytically.

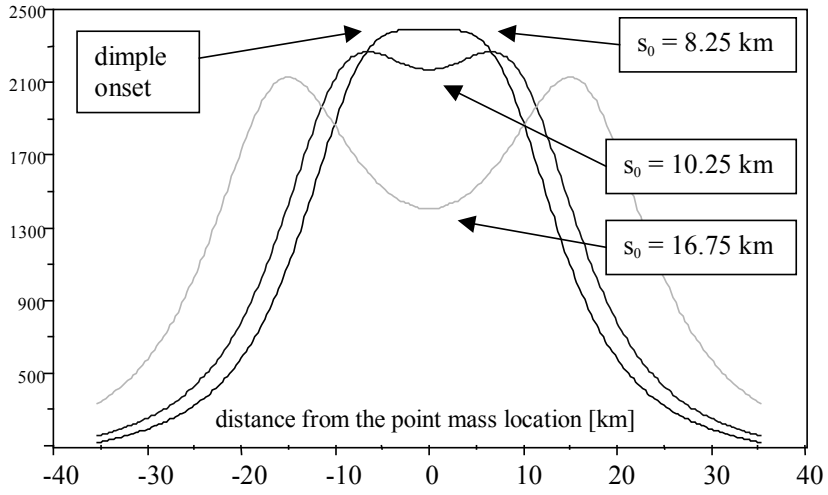

Fig. 2. Three illustrative snapshots from the animated dZ/ds_0 sequence generated by one point mass placed at depth $d = 10$ km. The $w(s) = \text{const} = 1$ was the kernel of the truncation filter for producing the above sequence. The dimple pattern sets on at instant $s_0^* = 8.25$ km $\pm$ 250 m (250 m is the numerical step in the truncation parameter when computing the sequence). Horizontal axis is distance from the point mass location projected onto the surface, in kilometers.

As for the approximation of the gravity anomaly by the vertical component of the gravity disturbance, we have assessed it by numerical experiments (computer simulation) from the viewpoint of the relationship between the instant of the dimple onset and the depth of the point mass. Similarly to computer simulations for the vertical component of the gravity disturbance generated by the point mass, we perform computer simulations for the gravity anomaly (eqn.(9)) generated by the point mass. Numerical experiments show, that when using the gravity anomaly, the relationship between the instant of the dimple onset and the depth of the point mass deviates from the linear relationship derived when using the vertical component of the gravity disturbance. The shallower the point and the greater its mass the greater the deviation from the relationship $s_0^* \doteq 0.82\, d$. For example for a point mass at depth 1 km with a mass such, that it generates geoid with amplitude of its height 100 meters, $s_0^* \doteq 0.9375\, km$. For this point mass the error in the determination of its depth from the dimple onset ($d \doteq 1.22\, s_0^*$) caused by the said approximation would amount to about 144 meters. However, a point mass at depth 1 km generating a 100 meter geoidal feature is unrealistic. When choosing the mass of the point placed at depth 1 km such, that it generates geoid with amplitude 1 m, then $s_0^* \doteq 0.82\, km$, which is the same as in the case of the vertical component of the gravity disturbance. Let us denote the amplitude of the geoid (the maximum height of the geoidal feature) generated by a point

mass at depth d by N^a. Numerical experiments have shown, that for realistic point mass anomalies, under which we understand that $N^a/d \le 10^{-4}$, the approximation of the gravity anomaly by the vertical component of the gravity disturbance has practically no impact on the relationship between the depth of the point mass and the instant of the dimple onset. We conclude that for realistic point masses the truncation filtering methodology gives same results (depth determination) when using the vertical component of the gravity disturbance, as if the rigorous gravity anomaly was used.

3.1.2. Dimple onset – analytical derivation

The vertical component of the gravity disturbance generated by a point mass evaluated at point Q is given by eqn. (12). By denoting the distance between the computation point P and the projection of the point mass location onto the reference plane, point O, by ρ, we can express the gravity anomaly approximated by the vertical component of the gravity disturbance as follows (cf. Fig. 1)

$$\Delta g(r) \doteq \frac{\kappa m d}{\left(d^2 + s^2 + \rho^2 - 2s\rho\cos\alpha\right)^{3/2}}, \tag{13}$$

where α is the angle between the integration point Q and the point mass projected onto the boundary plane O, as viewed from the computation point P.

The instant of the dimple onset is the particular value of the planar truncation parameter at the moment of the curvature change of the first derivative of Z right above the point mass and hence is governed by the following equation (compare also with eqn.(7) in *Vajda and Vaníček, 1999*)

$$\frac{\partial^2}{\partial\rho^2}\left(\frac{dZ^{s_o}}{ds_o}(s = s_o, \rho)\right)\Bigg|_{\rho=0} = 0 \text{ satisfied by } s_0 = s_0^*. \tag{14}$$

By taking the first derivative of Z with respect to s_0 we arrive at (cf. eqn.(3))

$$\frac{dZ^{s_0}}{ds_0}(x_P, y_P) = w(s_0)\, s_0 \int_0^{2\pi} \Delta g(s = s_0, \alpha) d\alpha . \tag{15}$$

After substituting it back into eqn.(14), the governing equation for the dimple onset attains the form of

$$\int_0^{2\pi}\left(\frac{\partial^2}{\partial\rho^2}\Delta g(s = s_0, \rho, \alpha)\right)\Bigg|_{\rho=0} d\alpha = 0 , \tag{16}$$

since either $s_0\, w(s_0) \neq 0$, when the kernel has no node, or else if $w(s_0) = 0$, the node of the kernel is not the solution governing the instant of the dimple onset, rather it governs the instant when the whole surface of the first derivative of Z becomes zero, which is the instant when the whole sequence changes polarity (flips up-side-down). This going

through zero and flipping up-side-down of the dZ/ds_0 sequence may over-ride some pattern development in the sequence and this is the reason why we strongly recommend to use kernels with no node only. By examining eqn.(16) we also note, that the onset of the dimple pattern is a consequence of the truncation of the integration domain in the truncation filter, and does not depend at all on the kernel $w(s)$ of the truncation filter. This is an important fact.

When substituting for the gravity anomaly in eqn.(16) from eqn.(13), the dimple onset governing equation becomes

$$\frac{3\kappa m d}{\left(d^2+s_0^2\right)^{5/2}}\int_0^{2\pi}\left(\frac{5s_0^2\cos^2\alpha}{d^2+s_0^2}-1\right)d\alpha=0 \text{ satisfied by } s_0=s_0^*, \tag{17}$$

and after all the required development, also realizing, that the instant of the dimple onset is independent of the mass of the point anomaly, we arrive at

$$s_0^*=\sqrt{\frac{2}{3}}d\,. \tag{18}$$

Equation (18) proves theoretically that the depth of the point mass embedded in the horizontally infinite layer, which produces the dimple pattern in the sequence of the first derivative of Z, depends linearly on the instant of the dimple onset as $d=\sqrt{1.5}\ s_0^*$.

4. THE 3-D TRUNCATION FILTERING FOR A SPHERICAL MODEL

Suppose that the gravity data are referenced to a spherical boundary surface, to the reference sphere of radius R, then the need arises to formulate the truncation filtering for a spherical model as follows:

$$Z^{s_0}(\varphi_P,\lambda_P)=R\int_0^{s_0}\int_0^{2\pi}\Delta g(\varphi,\lambda)w(s)\sin\left(\frac{s}{R}\right)d\alpha\,ds\,, \tag{19}$$

where s is the *radial* distance between the computation point P (given by its latitude φ_P and longitude λ_P) and the point of evaluating the gravity anomaly Q (given by its latitude φ and longitude λ),

$$\cos\left(\frac{s}{R}\right)=\sin(\varphi_P)\sin(\varphi)+\cos(\varphi_P)\cos(\varphi)\cos(\lambda-\lambda_P)\,, \tag{20}$$

and where $d\sigma_Q=R\sin\left(\frac{s}{R}\right)ds\,d\alpha$ is the integration surface element.

Also the truncation parameter s_0 now has the nature of radial distance, being called the *radial* truncation parameter. Everything else remains the same story as for the planar model.

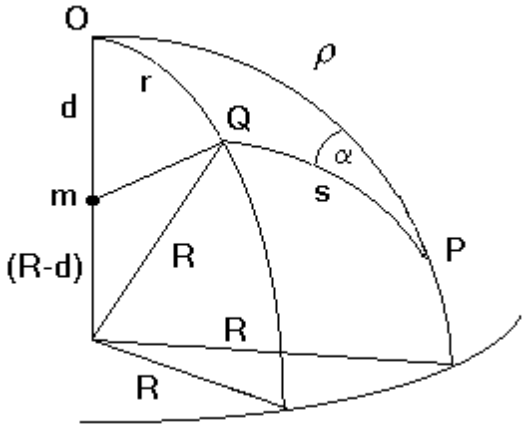

Fig. 3. The anomalous point mass *m* embedded at depth *d* in the homogenous massive sphere of radius *R*.

4.1. One point mass

We shall again examine the model case of one point mass anomaly. Having the point mass *m* placed at depth *d* in a homogeneous massive sphere of radius *R*, as illustrated in Fig. 3, where *r* is the radial distance between the projection of the point mass onto the spherical boundary (point O) and the point of evaluation of the gravity anomaly (point Q), the gravity anomaly generated by such point mass, again approximated by the vertical component of the gravity disturbance, at point Q reads

$$\Delta g(\mathrm{Q}) = \Delta g(\varphi,\lambda) = \Delta g(r) \doteq \kappa m \frac{R - (R-d)\cos\left(\frac{r}{R}\right)}{\left[(R-d)^2 + R^2 - 2(R-d)R\cos\left(\frac{r}{R}\right)\right]^{3/2}}. \qquad (21)$$

The gravity anomaly is transformed by our truncation filter (eqn.(19)) into the *Z* and dZ/ds_0 sequences, exactly as it was in the above section for the planar model. As we would expect, the *Z* and dZ/ds_0 sequences (not presented graphically here) very much resemble their counterparts of the planar model. The dZ/ds_0 sequence displays a dimple pattern. The story repeats here (realizing that all distances are radial and the truncation parameter is radial, too), except for one substantial fact. The instant of the dimple onset is no longer related to the depth of the point mass according to eqn.(18). A new relationship between the dimple pattern onset and the depth of the point mass must be established.

4.1.1. Dimple onset – computer simulation

Computer simulations, using the vertical component of the gravity disturbance as an approximation to the gravity anomaly (cf. section 3.1.1), for several different depths and masses (such that the amplitude of the surface of the geoidal height would not exceed 100 meters) of the point mass have revealed, that, although the shape of the Z quantity and of its first derivative, and hence the shape of the dimple pattern, depends on the depth of the point mass (and also on the choice of the kernel), and is slightly different from the shape of that for the planar model, the instant of the dimple onset is independent of the mass of the point (and of the choice of the kernel). This fact is justified below analytically. The instant of the dimple onset no longer depends linearly on the depth of the point mass. Its dependence on depth, established by computer simulations, is presented in Fig. 4.

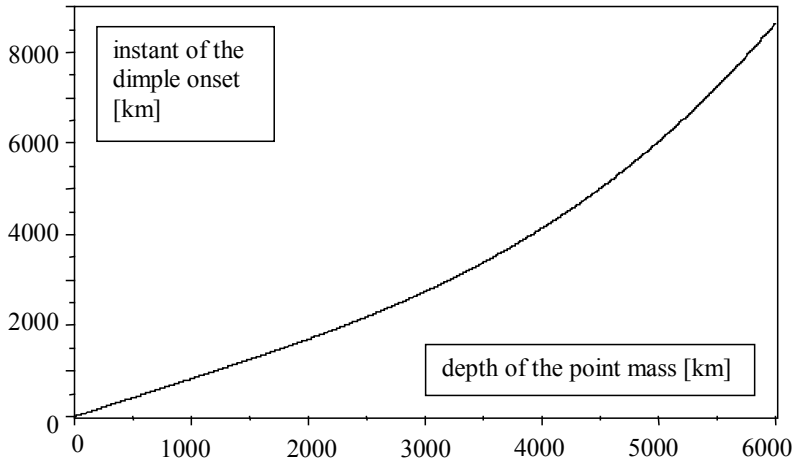

Fig. 4. The relationship between the instant of the dimple onset and the depth of the point mass compiled by computer simulations for several discrete depths of the point mass and interpolated by cubic splines.

4.1.2. Dimple onset – analytical derivation

By denoting the radial distance between the computation point P and point O by ρ, we can express the gravity anomaly at point Q (eqn. (21)), with the help of spherical trigonometry as follows (cf. Fig. 3)

$$\Delta g(\rho,s,\alpha) \doteq$$

$$\doteq \kappa m \frac{R-(R-d)\left(\cos\left(\frac{\rho}{R}\right)\cos\left(\frac{s}{R}\right)+\sin\left(\frac{\rho}{R}\right)\sin\left(\frac{s}{R}\right)\cos\alpha\right)}{\left[(R-d)^2+R^2-2(R-d)R\left(\cos\left(\frac{\rho}{R}\right)\cos\left(\frac{s}{R}\right)+\sin\left(\frac{\rho}{R}\right)\sin\left(\frac{s}{R}\right)\cos\alpha\right)\right]^{3/2}} \tag{22}$$

where α is the angle between the integration point Q and the point mass projected onto the boundary sphere as viewed from the computation point P.

The instant of the dimple onset is again the particular value of the radial truncation parameter at the moment of the curvature change of the first derivative of Z right above the point mass, and hence is governed by the following equation, analogical to eqn.(14), here ρ being the radial rather than planar distance

$$\frac{\partial^2}{\partial\rho^2}\left(\frac{dZ^{s_0}}{ds_0}(s=s_0,\rho)\right)\Bigg|_{\rho=0} = 0 \text{ satisfied by } s_0 = s_0^*. \tag{23}$$

Taking the first derivative of Z results in

$$\frac{dZ^{s_0}}{ds_0}(\mathrm{P}) = R\sin\left(\frac{s_0}{R}\right)w(s_0)\int_0^{2\pi}\Delta g(s=s_0,\alpha)\,d\alpha\,.$$

Following the same procedure as for the planar model, with the same story about the node of the kernel, i.e. the "$\sin(s_0/R)w(s_0)=0$" solution, we get

$$\int_0^{2\pi}\left(\frac{\partial^2}{\partial\rho^2}\Delta g(\rho,s=s_0,\alpha)\right)\Bigg|_{\rho=0} d\alpha = 0\,, \text{ satisfied by } s_0 = s_0^*. \tag{24}$$

By substituting for the gravity anomaly from eqn. (22) into eqn. (24), and performing all the required and tedious developments, we arrive at the following equation for the relation between the instant of the dimple onset and the depth of the point mass anomaly in case of a spherical model, and for the gravity anomaly, which is truncation filtered, being approximated by the vertical component of the gravity disturbance

$$f(R,d,s_0) = u(R,d,s_0)+v(R,d,s_0)+t(R,d,s_0) = 0 \text{ satisfied by } s_0 = s_0^*, \tag{25}$$

where

$$u(R,d,s_0) = 2\frac{R-d}{R^2}\cos\left(\frac{s_0}{R}\right)\left[(R-d)^2+R^2-2R(R-d)\cos\left(\frac{s_0}{R}\right)\right]^3,$$

$$v(R,d,s_0) = (-6)\left[R-(R-d)\cos\left(\frac{s_0}{R}\right)\right]$$
$$\frac{R-d}{R}\cos\left(\frac{s_0}{R}\right)\left[(R-d)^2+R^2-2R(R-d)\cos\left(\frac{s_0}{R}\right)\right]^2,$$

$$t(R,d,s_0) = 15\,(R-d)^2\sin^2\left(\frac{s_0}{R}\right)\left[R-(R-d)\cos\left(\frac{s_0}{R}\right)\right]$$
$$\left[(R-d)^2+R^2-2R(R-d)\cos\left(\frac{s_0}{R}\right)\right].$$

This is a different result compared to that, when the problem is formulated on the plane. We will seek the solution $s_0^* = s_0^*(d)$ of eqn. (25) for a fixed R graphically, cf. Fig. 5.

The results obtained by this analytical derivation match the results acquired by computer simulations.

For a reference sphere of radius of about that of the earth and depths up to 100 km, the dependence is practically linear. The smaller the depth, the closer the $d = d(s_0^*)$ dependence is to $d = \sqrt{1.5}\, s_0^*$. When processing synthetic gravity data referenced to a sphere with radius R of roughly the radius of the earth, and having anomalous point

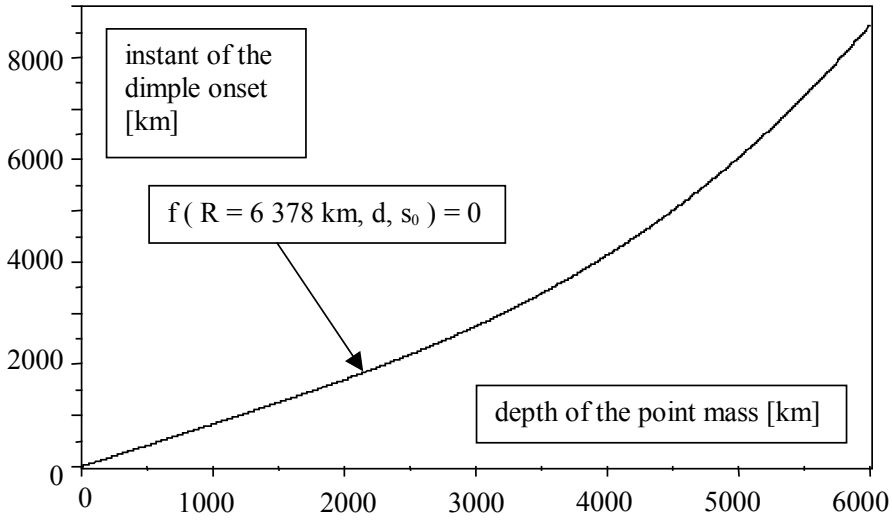

Fig. 5. The relationship between the instant of the dimple pattern onset and the depth of the point mass for a spherical model (R = 6 378 km) obtained from the analytical derivation by graphically solving the dimple onset defining equation $f(R = 6378 \text{ km}, d, s_0) = 0$.

masses no deeper than some 100 km, we can accurately enough replace the spherical model with the planar model (replace radial distances with planar distances, and replace radial truncation parameter with planar truncation parameter), and replace eqn.(25) with $d = \sqrt{1.5}\, s_0^*$.

In case of the spherical model we evaluate the convolution integral – the truncation filter – in spherical coordinates and display the results mapped onto the tangent plane of the projection of the point mass onto the reference sphere. In a spherical model it is also possible to evaluate convolution integrals in a moving tangent plane, which introduces a planar approximation to the spherical problem, cf. for instance *Grafarend and Krumm (1996;1998)*. More about the use of the planar approximation in spherical geodetic or geophysical problems may be found in e.g. *Bellaire (1972), Groten (1965;1966a,b)*, *Jordan (1972), Shaofeng and Zhang (1993)*.

5. THE TRUNCATED STOKES TRANSFORM AS A TRUNCATION FILTER

When the truncation filter is formulated for a spherical model (cf. eqn.(19)), and the kernel chosen as

$$w(s) = \frac{1}{4\pi\gamma R} S\left(\frac{s}{R}\right), \tag{26}$$

where S is the Stokes function (*Stokes, 1849*), γ is normal earth gravity, and R is mean earth's radius, then the truncation filter becomes the Truncated Stokes Transform (*Vajda and Vaníček, 1999*), the Z quantity becomes the *truncated geoidal height*, the Z sequence becomes the TG sequence (the truncated geoid sequence) [ibid] and the dZ/ds_0 sequence becomes the DTG sequence (the first derivative of TG with respect to the truncation parameter sequence) [ibid]. *Vajda and Vaníček (1999)* derived the instant of the dimple onset setting on in the DTG sequence (eqn.(32) in [ibid]) for one point mass anomaly m embedded at depth d in a homogenous massive sphere approximating the earth. In that derivation the gravity anomaly producing the DTG sequence was defined rigorously from the fundamental gravimetric equation, using a disturbing potential with proper mass and proper center of mass. This rigorous definition of the gravity anomaly caused, that the instant of the dimple onset was not only dependent on the depth of the point mass, but also on its mass. However, the dependence on mass was very minute. After neglecting the dependence on mass m (cf. [ibid]), the relationship between the instant of the dimple onset and the depth of the point mass becomes linear and reads (for R = 6 378 km)

$$d\ [km] \doteq 135.82\ [km/\text{arc deg}]\ \psi_0^*\ [\text{arc deg}], \tag{27}$$

where ψ_0 is the (polar) truncation parameter [in arc degrees] and relates to the radial truncation parameter as $\psi_0 = s_0/R$, while the asterisk denotes the instant of the onset. Thus eqn. (27) can be rewritten (replacing the arc degrees with radians and putting R = 6 378 km) in terms of the radial truncation parameter as

$$\text{(a) } d \doteq 1.22\, s_0^* \text{ , or (b) } s_0^* \doteq 0.82\, d \ . \tag{28}$$

Equation (28) is in agreement with eqn. (18). It is also in agreement with eqn. (25) for shallow depths in its linear approximation. This actually means, that in a spherical model, and for shallow point masses, the rigorous gravity anomaly may be approximated by the vertical component of the gravity disturbance, and the relationship between the instant of the dimple onset and the depth of the point mass is linear and identical with that of eqn. (18).

6. CONCLUSIONS

In Sections 3 and 4 we have mathematically formulated the truncation filtering methodology on the boundary (reference) plane and on the boundary (reference) sphere respectively. The truncation filtering can be used as the aid in the gravimetric inversion or gravity data interpreting. The truncation filtering methodology consists of transforming the gravity anomaly given on the reference plane or sphere into the Z and dZ/ds_0 sequences for a series of systematically varied values of the truncation parameter. Both these sequences (of the Z and dZ/ds_0 surfaces) are animated with respect to varying the value of the truncation parameter. Patterns that are signatures of the individual features of the anomalous mass distribution appear in the sequences. These patterns can be used for interpreting the mass distribution that generates the original gravity data. Here we present only the fundamental concept of the truncation filtering methodology, as an inversion or interpretation tool, represented by inverting the gravity anomaly generated by one point mass anomaly in terms of its depth. The model of one point mass anomaly produces the dimple pattern in the dZ/ds_0 sequence. The relation between the instant of the dimple onset and the depth of the point anomaly is derived analytically for both the planar and spherical models – Sections 3.1.2 and 4.1.2. The derivation matches the results of computer simulations. Inverting gravity anomalies of point masses may find some use in physical geodesy, but likely very limited use in applied gravimetry. Computer simulations will be used to study patterns of more realistic geologic mass distribution features to develop the pattern recognition skills, and to establish relations between onsets of patterns and depth estimates of the individual geological features. Attention will be also paid to the choice of kernels of truncation filters.

When using the truncation filtering methodology and dealing with shallow mass anomalies (depths up to 100 km in case of mean earth), the rigorous gravity anomaly may be approximated by the vertical component of the gravity disturbance and the spherical model may be replaced by the planar model.

Acknowledgements: The use of the SCILAB freeware by INRIA is acknowledged.

Received: January 31, 2001; *Accepted: December 13, 2001*

References

Bellaire R.G., 1972. *A discussion of flat earth statistical models for the gravity disturbances and their application*. Report 1972, The Analytic Sciences Corporation, Reading, Mass.

Grafarend E.W. and Krumm F., 1996. The Stokes and Venig-Meinesz functionals in a moving tangent space. *J. Geodesy*, **70**, 696–713.

Grafarend E.W. and Krumm F., 1998. The Abel-Poisson kernel and the Abel-Poisson integral in a moving tangent space. *J. Geodesy*, **72**, 404–410.

Grant F.S. and West G.F., 1965. *Interpretation Theory in Applied Geophysics*, McGraw-Hill Book Co., New York.

Groten E., 1965. *A gravity prediction using mean anomalies*. Report 47, Dept. of Geodetic Science, the Ohio State University, Columbus, Ohio, U.S.A.

Groten E., 1966a. *Analytical continuation of gravity using orthogonal functions*. Report 53, Dept. of Geodetic Science, the Ohio State University, Columbus, Ohio, U.S.A.

Groten E., 1966b. *On the derivation of surface gravity anomalies from airborne measurements*. Report 53, Dept. of Geodetic Science, the Ohio State University, Columbus, Ohio, U.S.A

Jordan S.K., 1972. Self-consistent statistical models for the gravity anomaly, vertical deflections, and undulation of geoid. *J. Geophys. Res*., **77**, 3660–3670.

Kellogg O.D., 1929. *Foundations of Potential Theory*. Springer, Berlin.

Shaofeng B. and Zhang K., 1993. The planar solution of geodetic boundary value problem. *Manuscripta Geodaetica*, **18**, 290–294.

Stokes G.G., 1849. On the Variation of Gravity at the Surface of the Earth. *Trans. Cambridge Philosophical Society*, **VIII**, 672–695.

Vajda P. and Vaníček P., 1997. On Gravity Inversion for Point Mass Anomalies by Means of the Truncated Geoid. *Stud. geophys. geod.,* **41**, 329–344.

Vajda P. and Vaníček P., 1999. Truncated geoid and gravity inversion for one point-mass anomaly. *J. Geodesy*, **73**, 58–66.

Vaníček P. and Krakiwsky E.J., 1986. *Geodesy: The Concepts*, 2nd rev. edition, North-Holland P.C., Elsevier Science Publishers, Amsterdam.

Vaníček P., Huang J., Novák P., Pagiatakis S., Véronneau M., Martinec Z. and Featherstone W.E., 1999. Determination of the boundary values for the Stokes-Helmert problem. *J. Geodesy*, **73**, 180–192.